An analysis method to evaluate the added resistance in short waves considering bow wave breaking

Choi, BongJun; Huijsmans, Rene

Publication date
2016

Document Version
Final published version

Published in
Proceedings of the12th International Conference on Hydrodynamics-ICHD 2016

AN ANALYSIS METHOD TO EVALUATE THE ADDED RESISTANCE IN SHORT WAVES CONSIDERING BOW WAVE BREAKING

BongJun Choi and Rene H.M. Huijsmans
Delft University of Technology
Mekelweg 2, 2628 CD Delft, The Netherlands
b.choi@tudelft.nl

ABSTRACT: A bow wave breaking is one of the most prominent factors to be considered regarding the nonlinearity of added resistance for a ship. Considering the stability of the bow wave breaking, which is mostly influenced by the ship speed and the waterline entrance angle, can enhance understanding of the nonlinearity. New transfer function containing the ship speed is proposed to make a better representative of the nonlinearity. This method is evaluated with the model test data of the Fast Displacement Ship (FDS) under the short waves condition ($\lambda/L = 0.4$). This study has shown that new transfer function can be an efficient analysis method of the ship performance prediction offering intuitive consistency with proposed residual resistance concept. The findings lead to better understanding the nonlinearity considering bow wave breaking.

1. INTRODUCTION

A bow wave, generated by a ship advancing on the free surface is an important component of the resistance. This bow wave shows a stable form for a fine bow or an unstable disturbance for a blunt bow of a ship. In a calm sea, when the bow wave breaks, this breaking is considered in a part of the residual resistance. However, in waves, the influence of the bow wave breaking on the added resistance is not clearly defined. This is an important aspect of the uncertainty.

The resistance prediction for the calm sea is a crucial process for estimating the performance of a ship. The experiment accurately measures the resistance and extrapolated to those of the full ship. The numerical prediction also shows good agreement [1]. However, added resistance is not predicted as the similar accuracy of the calm water resistance. Traditionally, this sea-going performance is empirically decided and applied as a sea margin. As a tool for control CO_2 emission from a ship, International Maritime Organization (IMO) issued the Energy Efficiency Design Index (EEDI). Added resistance is a part of this index considering a weather factor [1]. However, this factor of an actual sea-going performance is reserved for use in this index calculation, due to the absence of an appropriate evaluation method [2].

The added resistance prediction based on the motion response of a ship in waves showed reasonable agreement with the experiment data in accordance with fair prediction of the motion response, such as the momentum conservation method [3, 4], the radiated energy method [5], the pressure integration based on Rankine panel method [6, 7] and the asymptotic formula [8, 9]. However, as a new generation of a ship, the ship length is growing, and those ships have a high probability to sail in short waves with negligible wave-induced motion. The stationary motion induces unreliability of the added resistance prediction. The diffraction and the reflected wave become major contributors.

Numerous research is recently published to improve the accuracy of the short wave problem, such as the experiment based correction [10], the alternative method of a ray theorem [11], the combined method that associate the method based on the radiated energy method [5] with asymptotic formula [8, 12] or with semi-empirical [10], the extended integral equation method

[13], the Rankine panel method and extended RANSE [14], the Rankine panel method and FV-based Cartesian-grid method [15] and CFD method [16, 17]. However, those numerical methods are limited to the particular problem due to the complexity, such as highly representative nonlinear wave effects and grid limitation to capture small waves without aliasing error. Furthermore, a rational evaluation method for the bow wave breaking is not defined under the given hullform.

The important feature of this study is to find representative factors on a bow wave breaking through previous research results and present a new transfer function with applying the residual resistance concept to improve the interpretation of the nonlinearity considering the stability of bow wave breaking. This method is evaluated with the model test data of three Fast Displacement Ships (FDS) under the short waves condition ($\lambda/L = 0.4$).

2. BOW WAVE BREAKING

The bow wave breaking can be classified as the breakers type on the crest of the bow wave although the boundary is unclear: stable plunging breakers or unstable spilling breakers. The plunging breakers are used to refer to an overturning spray wave, which curls over and drops onto the free-surface. The spilling breakers refer to a relatively unstable wave breaking with a turbulent white bubble on the crest.

Maxeiner [18] investigated on the physics of bow wave breaking for the fine bow by using two dimensions plus time (2D+T) approximation with flexible wave board. He classified the breakers type into plunging and spilling. According to his research, the breakers type have a close relationship with the motion of the contact point of wave board on the water. This contact point represents the entrance angle and the speed of a ship. Moreover, breakers type are occasionally alternated each other even for the same condition. This shows that a transient region exists. Karion [19] implies the transition in the form of the bow wave breaking as a function of the ship speed in their experimental research for simple wedge geometry.

The stability of the bow wave

Noblesse et al. [20] introduced a boundary of stability on the crest of a ship bow waves in calm water condition through the simple analytical relation with equation (1). In this relation, primary fundamental considerations, such as the Bernoulli relation and dimensional analysis for a non-bulbous wedge-shaped bow are used with the experimental approximation.

$$F_D = \frac{4.4}{(1-q_b^2)} \frac{tan\alpha_E}{cos\alpha_E} - 1 \tag{1}$$

where q_b is the flow total velocity at a bow wave crest and α_E is the entrance angle and F_D is the ship draft D based Froude number ($F_D = U/\sqrt{(gD)}$). Fig. 1 depicts this boundary for the various number of the flow velocity on the crest q_b.

In the research of Noblesse et al. [20], the major aspects that affect the stability of the bow wave crest are the depth-based Froude number (F_D) and the waterline entrance angle ($2\alpha_E$). Fig. 1 shows that when the test condition is on the left-hand side of the boundary, the bow wave is expected to be stable form. If the bow wave breaks in this stable condition, plunging type overturning detachment is to be expected. On the other hand, when the condition is on the right-hand side of the boundary, unstable (correspond to 'unsteady' in his description) spilling type of bow wave is to be expected.

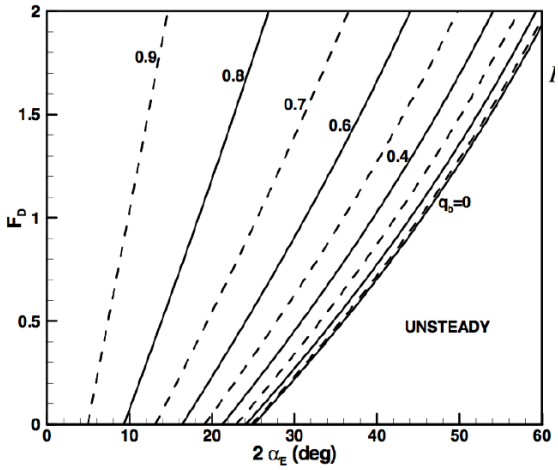

Figure 1 - Stability boundary of the bow wave from equation (1) **for the various number of the flow velocity on the crest** q_b **(Noblesse et al. [20]).**

Influence on the resistance according to the type of breakers

Rapp and Melville [21] analyzed the effect of deep-water wave breaking by the experimental approach concerning the loss of excess momentum flux. The momentum flux is the ratio of squared wave height of before and after breaking. They observe: 'The loss of excess momentum flux and energy flux from the wave group was measured and found to range from 10% for single spilling breakers to as much as 25% for plunging breakers.' There is a different loss of momentum flux according to the type of the breakers. For the wave itself, spilling breakers have smaller energy loss with preserving the wave height after breaking. In other words, disturbed energy remains more on the wave itself as an unstable form and increase instability.

The spilling breakers occur in front of the ship stem and disturb the near hull flow field with growing the turbulence. Kayo [22] explained the spilling related resistance increases for a blunt bow with a shear flow on the free surface. He showed that the increased shear flow on the free surface with the same direction of the ship induces a higher residual resistance. The reflected bow wave that induces forward spilled waves over the free surface generates the similar effect with the forward shear flow. As a result, The increased shear flow causes a higher residual resistance.

The bow wave breaking in short waves of head sea condition

A ship that advances in short waves in head sea condition appears stationary with no motion response of heave and pitch. In this stationary state, bow wave is affected by the incident wave upon the steady bow wave that inherited the interaction between the hullform and the ship speed. This affection of the incident wave changes the total velocity of the crest of the bow wave and the appearance of the bow wave. The stability of the bow wave crest is an important aspect to be considered. When the bow wave breaks, under the stable condition, the breakers type may have the form of stable plunging with an overturning detachment of bow wave. On the other hand, under the unstable bow wave, spilling with turbulent disturbance of near hull flow field is induced.

A linear based potential formulation is used and further developed to gain insights into the factors that affect added resistance based on the formulation of the Van't Veer [23]. Forces on the hull surface for instantaneous hull wetted surface S can be obtained by integrating the

pressures over the instantaneous hull wetted surface. Under the assumption that no motion response in short waves, we can leave out the terms that have motion response. This leads to abbreviated equation as follows:

$$\left\langle \vec{F}^{(2)} \right\rangle = \left\langle \frac{1}{2}\rho g \int_{wl} {\zeta_u^{(1)}}^2 \vec{n} l - \frac{1}{2}\rho \iint_{S_0} \nabla\varphi^{(1)} \cdot \nabla\varphi^{(1)} \vec{n} dS \right\rangle \tag{2}$$

where S_0 represents the wetted surface of the mean body and *wl* represents the waterline. $\vec{n}$ is the normal vector of the *S*, ρ is the fluid density, ζ_u is the unsteady wave height and φ is the unsteady potential.

In this stationary condition, the relative wave height distribution at the waterline of the ship and the velocity-squared term are the key aspects of the added resistance calculation. Because the bow wave breaking appears periodic phenomenon and affects the near hull pressure field, a potential calculation approach using the pressure integration method for added resistance still have the possibility of improvement. An additional consideration regarding relative wave height and velocity disturbance can play a crucial role in this issue.

3. THE CONCEPT OF THE RESIDUAL ADDED RESISTANCE

Under the given hullform, the bow wave related representative factors are hullform, incident wave, and the ship speed. The hullform parameters such as the waterline entrance angle, flare, length, breadth, and depth are considered in the residual resistance C_r distribution along the Froude number Fn in calm water. The incident wave parameters such as amplitude and frequency affect the diffraction term, which is essential to solving the potential problem. The ship speed influences to the stability of the bow wave, the diffraction of the incident wave, and reflected wave. Thus, an analysis of the added resistance regarding the bow wave breaking requires being considered as a function of the ship speed.

Kuroda et al. [10] proposed a correction term of the slender body theory based on Maruo's formula, which is derived from the model test results considering the advancing ship speed, to improve the accuracy of the linear prediction. This hybrid calculation method showed reasonable agreement with the experimental data for the container ship.

The added resistance is traditionally considered as proportional to the square of the amplitude of the incident wave under the non-breaking condition [24]. The stability and breaking type of the bow wave breaking depends on the ship speed. We, therefore, propose new transfer function to improve the interpretation of the nonlinearity as a name of the 'residual added resistance (C_{ra}).' This proposed transfer function that provides a relationship with the perspective of the bow wave breaking influences on the added resistance, including the consideration of the ship speed and the amplitude of the incident wave.

$$C_{ra} = \frac{R_{aw}}{\frac{1}{2}\rho\zeta_a^2 U^2} \tag{3}$$

where R_{aw} is the measured added resistance, ρ is the water density, ζ_a is the amplitude of the incident wave and U is the ship speed. Whereas, a traditional quadratic transfer function is given by

$$C_{aw} = \frac{R_{aw}}{\frac{1}{2}\rho g B^2 \zeta_a^2 / L} \tag{4}$$

in which g is the acceleration of gravity, B is the maximum breadth of the waterline and L is the length between perpendiculars.

4. EXPERIMENT

Model tests of a Joint Industry Project on 1979-1989 [25] were carried out for the systematic series of fast displacement ship (FDS). The resistance in calm water and added resistance in waves with the motion responses were measured. Among these test results, three hullforms that have the same body plan, block coefficient C_b and breadth over draft ratio B/T were selected, but those hullforms have different length and breadth L/B ratio. This geometrical variation produces the different hullform, which has a different waterline entrance angle. The bodyplan and the main particulars are shown in Table 1 and Fig. 2.

Table 1 - The main particulars of three FDS hulls for FDS-20, FDS-11 and FDS-19.

	FDS-20	FDS-11	FDS-19
B/T	4		
C_B	0.35		
L/B	12	8	4
$2\alpha_E(^\circ)$	11.4	17.0	33.2

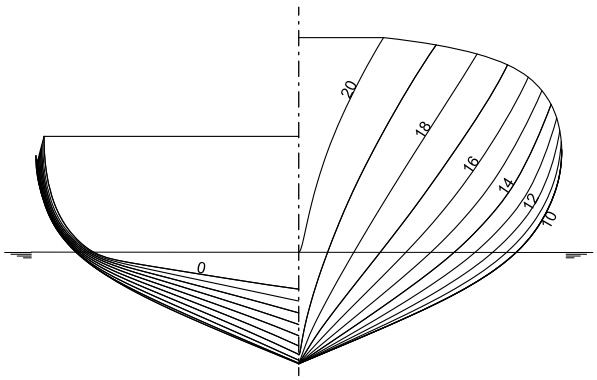

Figure 2 - Body plan of the three hullforms for FDS-20, FDS-11 and FDS-19.

The model test results are analyzed considering the influence of the bow wave breaking. The measured resistances of the three hullform in calm water are analyzed according to the two-dimensional method of International Towing Tank Conference in 1978 (ITTC-78) performance prediction method [26], which divide the total resistance C_t into the frictional resistance C_f and residual resistance C_r.

The total resistance coefficient is given as follows:

$$C_t = \frac{R_T}{\frac{1}{2}\rho S U^2} \tag{5}$$

where R_T is the total resistance, S is the wetted surface area and U is the ship speed.

The frictional resistance C_f comes from shear-stresses of the flow around the hullform. The frictional resistance is treated as the same with the measured resistance of flat plate, which has the same wetted surface area under the wave-free condition. The typical formula is offered by the International Towing Tank Conference in 1957 (ITTC-57).

$$C_f = \frac{0.075}{\{log(Rn) - 2\}^2} \tag{6}$$

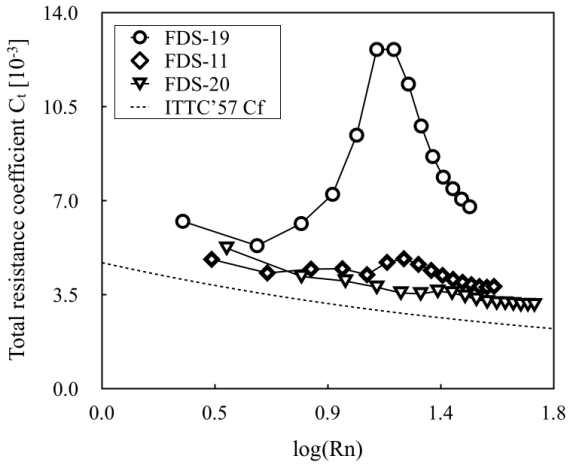

Figure 3 - Total resistance coefficients of each hullform of FDS-19, FDS-11 and FDS-20 along the $log(Rn)$ with the frictional resistance coefficient of ITTC-57.

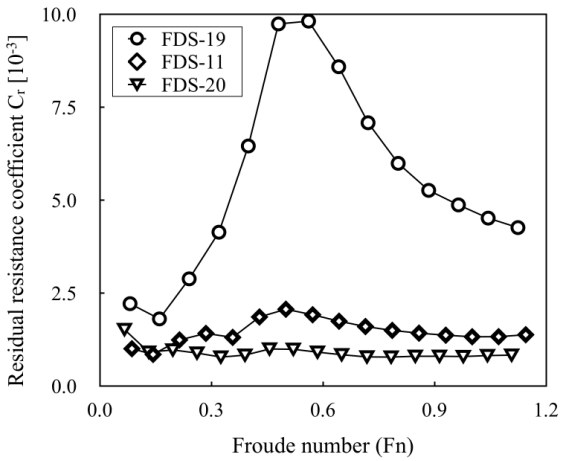

Figure 4 - Residual resistance coefficients of each hullform of FDS-19, FDS-11 and FDS-20 along with the Fround number Fn.

The rest resistance of the total resistance of the ship except the frictional resistance is the residual resistance C_r.

$$C_r = C_t - C_f \tag{7}$$

Fig. 3 depicts total resistance coefficients of each hullform of FDS-19, FDS-11, and FDS-20 along the $log(Rn)$ with frictional resistance coefficients of ITTC-57 of equation (6). This figure shows that the total resistances of each hullform appear with the big difference. Fig. 4 depicts residual resistance coefficients of each hullform. This figure reveals that each hullform has the different slope on $Fn < 0.5$. Moreover, three hullforms have the peak residual resistance coefficient at Fn = 0.5. Every residual resistance coefficient converges to a certain value of each hullform at the high-speed region as $Fn \to \infty$.

The added resistance for three ships in short waves of wavelength ratio $\lambda/L = 0.4$ was measured for the Fn = 0.285, 0.430, 0.570, 0.855, and 1.140. The response amplitude operator of heave and pitch approach to zero on this $\lambda/L = 0.4$ condition. Under this stationary condition, the added resistance are analyzed by traditional quadratic transfer function C_{aw} of equation (4) and present residual added resistance coefficient C_{ra} of equation (3).

Fig. 5 depicts experiment data with symbols of circle, diamond and counter-triangle stand for FDS-19, FDS-11, and FDS-20, respectively. The left of Fig. 5 depicts the quadratic transfer function C_{aw} regarding the Froude number for three ships. Although C_{aw} shows that the added resistance seems to have the proportional relation with the Froude number, any clear relationship cannot be established as the added resistance with the Froude number. The right of Fig. 5 depicts the residual added resistance coefficient C_{ra} with respect to the Froude number for three ships. In contrast to the C_{aw}, the residual added resistance coefficient C_{ra} shows a clearer relationship regarding the Froude number. Every residual added resistance coefficient decrease as the ship speed increases. On the right of Fig. 5, FDS-19 that has 33.2° of the waterline entrance angle ($2\alpha_E$) appears higher residual added resistance coefficient than those of others. These higher values correspond to having a high residual resistance in calm water in Fig. 4. The sudden breakdown point between Fn = 0.430 and Fn = 0.570 of FDS-19 is coincided with the crest value region of the residual resistance of FDS-19 on the Fig. 4.

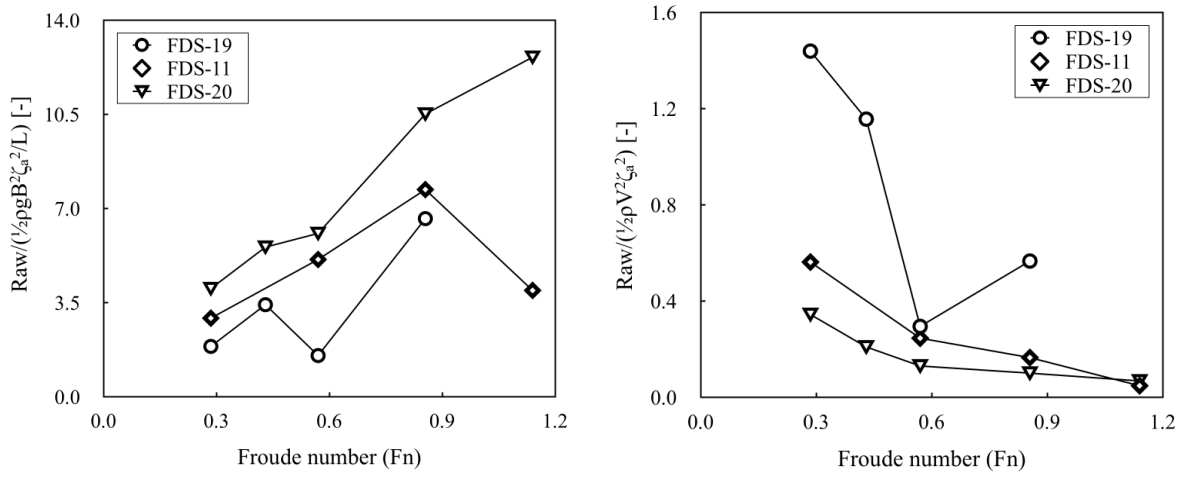

Figure 5 - Added resistance with the symbols of circle, diamond and counter-triangle stand for FDS-19, FDS-11 and FDS-20, respectively. The left figure depicts the quadratic transfer function C_{aw} with respect to the Froude number and the right of the residual added resistance coefficient C_{ra} with respect to the Froude number.

5. DISCUSSION

In calm water, the resistance is the resultant drag, which reflects the interaction between the hullform and the ship speed. Among the resistance components, the residual resistance was difficult to define as a simple relation function, because it appears differently according to the complex combination of the ship speed with the hullform parameters such as length, breadth, depth, entrance angle, flare angle. In contrast, the frictional resistance can be defined as a function of the wetted surface area and the ship speed. However, The relation between the bow wave breaking and the residual resistance may be explained with the stability of the bow the residual resistance wave breaking. In the Fig. 4, the residual resistance coefficient C_r increases with the larger relation than the square of the ship speed on $Fn < 0.5$ regions.

The increased slope depends on the waterline entrance angle of the ship, which is the important factor in the stability of the bow wave under the same body plan. This region can be defined as the development region of the bow wave, and the resultant residual resistance is larger than the relation of the square of the ship speed. As $Fn \rightarrow \infty$, residual resistance coefficient is converging to each own values. At this region, due to the strong plunging breaking, bow wave development is suppressed. The residual resistance becomes proportional to the square of the ship speed. These interpretations of the residual resistance with the ship speed and entrance angle are consistent with added resistance analysis by presented residual added resistance coefficient C_{ra}. On the right side of Fig. 5, the observed decreases in C_{ra} as ship speed increase could be attributed to the higher strength of overturning detachment that is stable plunging breaking. The big difference of C_{ra} as Fn increase for the FDS-19 can be explained by the change of the type of bow wave breaking, as the type of the stability changed from unstable to stable as ship speed increase.

Fig. 6 depicts the added resistance regarding the waterline entrance angle ($2\alpha_E$). The left of Fig. 6 depicts the traditional quadratic transfer function Caw and the right of Fig. 6 depicts the present residual added resistance C_{ra} with respect to the waterline entrance angle. This figure shows that the residual added resistance C_{ra} is proportional to the waterline entrance angle with a different slope for each ship speeds. The higher residual added resistance as the waterline entrance angle increase also can be explained by the difference in the stability of the bow wave,

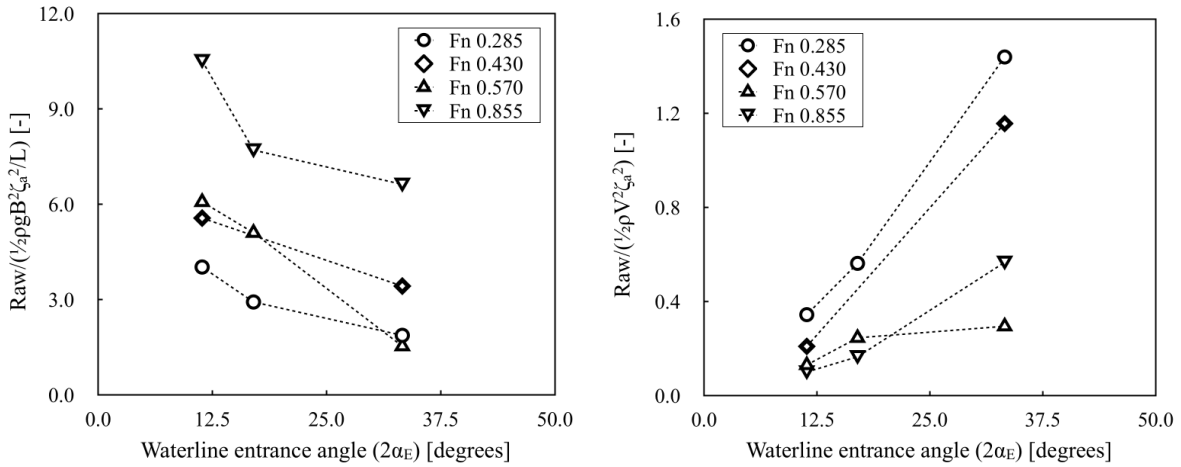

Figure 6 - the added resistance in terms of the waterline entrance angle ($2\alpha_E$). The left of figure depicts the traditional quadratic transfer function C_{aw} and the right of figure depicts the presented residual added resistance C_{ra} with respect to the waterline entrance angle.

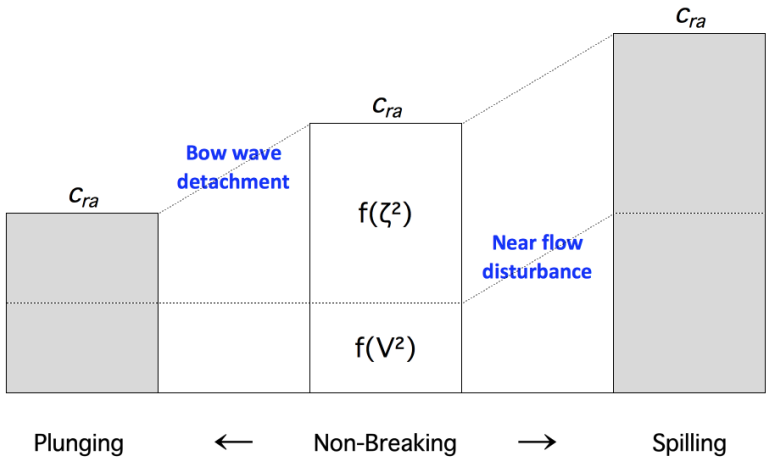

Figure 7 - Concept of the residual added resistance and its contribution on the added resistance

which is stable for the small waterline entrance angle and unstable as the waterline entrance angle increase. This investigation supports the hypothesis of Fig. 7 that slow speed and large entrance angle induce the unstable bow wave breaking. The stable plunging breaking induces detachment of the bow wave and the relative wave height related contribution might decrease. In contrast, the unstable spilling breakers induce turbulent disturbance around ship hullform and the velocity field related contribution may enlarge.

6. CONCLUSION

In this study, the added resistance in short waves is considered in the perspective of the stability of the bow wave and its breaking. The motion response is neglected in this analysis and this research only focus on the diffraction related bow wave breaking in head sea condition in short waves. The nonlinearity is induced by the bow wave breaking, which can be classified by the type of stable plunging and unstable spilling. The residual resistance in calm water, which inherited the hullform related parameters such as the waterline entrance angle, helps to understand

the stability of the bow wave. This stability of the bow wave affects the form of the bow wave breaking, and this breaking leads to the different contribution of the added resistance. Therefore, as the determinant of the stability of the bow wave, the consideration of the ship speed is essential to evaluate the added resistance in short waves under the given hullform. In this regard, the new transfer function with the residual added resistance concept is provided considering the ship speed. This ship speed consideration is also in agreement with the calm water resistance analysis. This residual added resistance concept in the Fig.7 intuitively describes the affection of the bow wave breaking on the added resistance. Further research question remains unanswered at present, such as a validation of the pressure field affection as the type of the bow wave breaking. These issues need to be undertaken.

7. ACKNOWLEDGEMENTS

The authors would like to thank the Maritime Research Institute Netherlands (MARIN) for making the model test results available.

REFERENCES

1. MEPC, I. (2011). Amendments to marpol annex vi on regulations for the prevention of air pollution from ships by inclusion of new regulations on energy efficiency for ships.
2. ITTC (2014). Seakeeping committee. final report and recommendations to the 27th ittc. *Proceedings of the 27th ITTC*.
3. Maruo, H. (1963). Resistance in waves. *Research on Seakeeping Qualities of Ships in Japan, The Society of Naval Architects of Japan 8*, 67–102.
4. Kashiwagi, M., T. Ikeda, T. Sasakawa, et al. (2010). Effects of forward speed of a ship on added resistance in waves. *International Journal of Offshore and Polar Engineering 20*(03).
5. Gerritsma, J. and W. Beukelman (1972). Analysis of the resistance increase in waves of a fast cargo ship. *International Shipbuilding Progress 19*(217).
6. Bunnik, T. H. J. (1999). *Seakeeping calculations for ships, taking into account the non-linear steady waves*. Ph. D. thesis, Delft University of Technology.
7. Kim, K.-H. and Y. Kim (2011). Numerical study on added resistance of ships by using a time-domain rankine panel method. *Ocean Engineering 38*(13), 1357–1367.
8. Fujii, H. and T. Takahashi (1975). Experimental study on the resistance increase of a ship in regular oblique waves. *Proc. of 14th ITTC 4*, 351–360.
9. Faltinsen, O., K. Minsaas, N. Liapis, and S. Skjørdal (1980). Prediction of resistance and propulsion of a ship in a seaway. *Proceeding of 13th Symposium on Naval Hydrodynamics Tokyo*.
10. Kuroda, M., M. Tsujimoto, T. Fujiwara, S. Ohmatsu, and K. Takagi (2008). Investigation on components of added resistance in short waves. *Journal of the Japan Society of Naval Architects and Ocean Engineers* (8), 171–176.
11. Sportelli, M. and R. Huijsmans (2012). Added resistance in short waves : a ray theory approach. *27th International Workshop on Water Waves and Floating Bodies*.
12. Guo, B.-j. and S. Steen (2011). Evaluation of added resistance of kvlcc2 in short waves. *Journal of Hydrodynamics, Ser. B 23*(6), 709–722.
13. Duan, W. and C. Li (2013). Estimation of added resistance for large blunt ship in waves. *Journal of Marine Science and Application 12*(1), 1–12.
14. Söding, H., V. Shigunov, T. E. Schellin, and O. el Moctar (2014). A rankine panel method

for added resistance of ships in waves. *Journal of Offshore Mechanics and Arctic Engineering 136*(3), 031601.
15. Seo, M.-G., K.-K. Yang, D.-M. Park, and Y. Kim (2014). Numerical analysis of added resistance on ships in short waves. *Ocean Engineering 87*, 97–110.
16. Sadat-Hosseini, H., P.-C. Wu, P. M. Carrica, H. Kim, Y. Toda, and F. Stern (2013). Cfd verification and validation of added resistance and motions of kvlcc2 with fixed and free surge in short and long head waves. *Ocean Engineering 59*, 240–273.
17. He, N. V. and Y. Ikeda (2014). Added resistance acting on hull of a non ballast water ship. *Journal of Marine Science and Application 13*(1), 11–22.
18. Maxeiner, E. (2009). *Physics of breaking bow waves*. Ph. D. thesis, Massachusetts Institute of Technology.
19. Karion, A., T. C. Fu, T. Waniewski-Sur, J. R. Rice, D. C. Walker, and D. A. Furey (2004). Experiment to examine the effect of scale on a breaking bow wave. Technical report, DTIC Document.
20. Noblesse, F., G. Delhommeau, M. Guilbaud, D. Hendrix, and C. Yang (2008). Simple analytical relations for ship bow waves. *Journal of Fluid Mechanics 600*, 105–132.
21. Rapp, R. and W. Melville (1990). Laboratory measurements of deep-water breaking waves. *Philosophical Transactions of the Royal Society A: Mathematical, Physical Engineering Sciences 331*, 735–800.
22. Kayo, Y. and K. Takekuma (1981). On the free-surface shear flow related to bow wave-breaking of full ship models. *Journal of the society of Naval Architectects of Japan 149*, 11–20.
23. Van't Veer, R. (1998). *Behaviour of catamarans in waves*. Ph. D. thesis, Delft University of Technology.
24. Pinkster, J. A. (1980). *Low frequency second order wave exciting forces on floating structures*. Ph. D. thesis, Delft University of Technology.
25. Kapsenberg, G., A. Aalbers, A. Koops, and J. Blok (2014). *Fast Displacement Ships*. Maritime Research Institute Netherlands.
26. ITTC (1999). Ittc performance prediction method.